Accelerating water exchange in Gd^{III}–DO3A-derivatives by favouring the dissociative mechanism through hydrogen bonding[i]

Loredana Leone[a], David Esteban-Gómez[b], Carlos Platas-Iglesias[b], Marco Milanesio[a] and Lorenzo Tei[a*]

[a] Dipartimento di Scienze e Innovazione Tecnologica (DiSIT), Università degli Studi del Piemonte Orientale "Amedeo Avogadro", Viale T. Michel 11, I-15121 Alessandria, Italy

[b] Centro de Investigacións Científicas Avanzadas (CICA) and Departamento de Química, Facultade de Ciencias, Universidade da Coruña, 15071 A Coruña, Galicia, Spain

Chemical Communications, volume 55, issue 4, pages 513–516, 14 January 2019
Submitted 25 October 2018, accepted 10 December 2018, first published 10 December 2018

How to cite:

L. Leone, D. Esteban-Gómez, C. Platas-Iglesias, M. Milanesio and L. Tei, Accelerating water exchange in Gd III -DO3A-derivatives by favouring the dissociative mechanism through hydrogen bonding, *Chem. Commun.*, 2019, **55**, 513–516. DOI: 10.1039/C8CC08556K.

Abstract

The Gd^{III}-complexes of DO3A-acetophenone and *ortho*- or *para*- hydroxyacetophenone ligands have been investigated to assess the effect of the presence of a phenol group on the relaxivity and on the water exchange rate of these potential MRI contrast agents. H-Bonding between the *ortho*-phenol(ate) groups and the water molecules involved in the dissociative exchange mechanism is shown to speed up the water exchange rate by stabilizing the eight-coordinate transition state.

Positive Magnetic Resonance Imaging (MRI) contrast agents (CAs) are paramagnetic metal complexes able to reduce the longitudinal relaxation time (T_1) of protons in their vicinity. Their efficiency (relaxivity, r_1) depends on several structural features of the complex, typically Gd^{III} or Mn^{II} derivatives, affecting the mode of interaction and magnetic coupling between the paramagnetic ion and the surrounding water molecules. Among them, the exchange rate (k_{ex}) of the water molecule coordinated to the metal center is a parameter of paramount importance.[1] Different strategies have been developed to control k_{ex} by modifying the structural and electronic features of Gd^{III} complexes.[2] For instance, it is well known that the GdDOTA complex and related systems may exist in solution as two diastereoisomers with either capped square antiprismatic (SAP) or capped twisted-square antiprismatic (TSAP) coordination polyhedra.[3] TSAP isomers present higher k_{ex} values than SAP isomers, due to a more pronounced steric hindrance around the coordinated water molecule.[4] Steric compression around the coordinated water molecule by modification of the ligand structure was also proved to be a successful strategy to accelerate water exchange. This was achieved by enlarging the size of the macrocycle in DOTA from a 12- to a 13-membered ring,[5] or by replacing an acetate arm by bulkier propionate or phosphonate arms in both macrocyclic[6] and non-macrocyclic ligands.[7] Water exchange in Gd^{III} complexes often proceeds through a dissociative mechanism and all strategies to increase k_{ex} rely on the destabilization of the reactant, typically a nine-coordinate $q = 1$ complex, with respect to the eight-

* lorenzo.tei@uniupo.it

coordinate transition state. Intramolecular hydrogen bonds between an H-bond acceptor present on a pendant arm and the coordinated water molecule (or the coordinated hydroxyl group) have been recently shown to increase the relaxivity of small molecular weight Gd^{III} complexes by restricting the rotation about the Gd–O_w bond or by accelerating proton exchange, respectively.[8,9] However, in these examples the H-bond formation did not involve modulation of k_{ex}.

In this work we present acetophenone, 2′- and 4′-hydroxyphenacyl derivatives of DO3A (DO3A-AP, DO3A-*o*HAP and DO3A-*p*HAP, DO3A = 1,4,7,10-tetraazacyclododecane-1,4,7-triacetic acid, Scheme 1) and a detailed study of the water exchange rates of the inner-sphere water molecules present in their Gd^{III} complexes. DO3A-AP and *p*-methoxy and *p*-dimethylamino substituted derivatives have already been described in the literature,[10] with the ketone-sensitised luminescence study on the corresponding Eu^{III} complexes. Herein, we will show that the presence of hydrogen-bond acceptors in the periphery of the coordinated water molecule accelerates dramatically the water exchange rate.

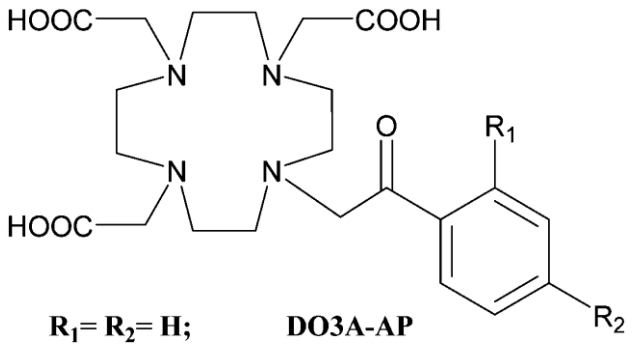

Scheme 1. Chemical structures of DO3A-AP and DO3A-HAP ligands.

The synthesis of DO3A-HAP chelators started from the reaction of DO3A(*t*Bu)$_3$ with *o*- or *p*-methoxy-2-bromoacetophenone followed by simultaneous deprotection of the methyl ether and the *tert*-butyl esters by using MeOH : HBr (aq) (1 : 1/v : v) into a microwave oven (60 °C, 70 W, 18 psi, 15 min) (Scheme S1 in ESI[i]). Complexation was accomplished by using the $LnCl_3$ salts (Ln^{III} = Gd, Eu) in water at pH 7. Free lanthanide ion excess was eliminated by precipitation and filtration of the hydroxide at basic pH. The pH dependence of the relaxivity (r_1) of GdDO3A-HAP complexes was measured to assess the possible change in r_1 with deprotonation of the phenol group. The graph of r_1*vs.* pH (Fig. S11, ESI[i]) shows no evident change in r_1 in the range of pH 2–12, whereas variable pH UV-vis measurements on DO3A-HAP ligands and on the corresponding Gd^{III}-complexes (Fig. S1–S3, ESI[i]) show a red shift of the absorption upon deprotonation of the phenol group. Similarly to other Gd^{III} complexes having a pH sensitive ligating group,[11] the differences in pK_a between ligands and Gd^{III} complexes (9.87 ± 0.09 for DO3A-*o*HAP; 8.67 ± 0.01 for DO3A-*p*HAP; 7.69 ± 0.04 for GdDO3A-*o*HAP; 7.01 ± 0.03 GdDO3A-*p*HAP) can be attributed to the delocalization of the anionic charge driven by the metal ion and formation of an enolate anion. Interestingly, for DO3A-*o*HAP and GdDO3A-*o*HAP the pK_a are higher due to the six-membered H-bonded ring between the carbonyl oxygen and the phenolic OH that reduces the electron withdrawing effect of the acyl group on pK_a (Fig. S2, ESI[i]).

The single crystal X-ray diffraction analysis (see ESI[i] for details) of GdDO3A-*o*HAP was carried out on a thin lamina and the crystal structure showed a $P2_1/c$ space group (CCDC 1875349[i]). The complex presents a SAP coordination around the Gd^{III} metal centre with a *cis*/*trans* disordered 2-hydroxyacetophenone moiety

with a 20/80 ratio (Fig. S4, ESI[i]), suggesting the presence of the two conformations in solution. The phenolic OH forms an intermolecular H-bond in *trans* conformation while an intramolecular water assisted H-bond is observed in the *cis* conformation (Fig. S5, ESI[i]). Notably, the Gd–O_{water} distance (2.37(1) Å) is rather short compared to similar structures in CCDC. Moreover, a peculiar porous network, filled by water molecules is formed because the phenol group stand out of the Gd-DO3A pseudo-spherical moiety (Fig. S6, ESI[i]).

A high-resolution ^{1}H NMR investigation on the EuDO3A-AP and EuDO3A-HAP complexes (pH 7 and 283, 298 and 310 K) allowed to determine the ratio between SAP and TSAP isomers in solution (Fig. S7–S10, ESI[i]).[12] In the case of EuDO3A-*o*HAP, the ^{1}H NMR spectra were recorded at two different pH, 3.5 and 9.5, in order to obtain the spectra of both protonated and deprotonated species. In all cases, a higher amount (72–78%) of SAP isomer was found.

A complete ^{1}H and ^{17}O NMR relaxometric study was carried out to obtain detailed information of the physicochemical properties of the complexes. The r_1 values for GdDO3A-AP and GdDO3A-HAP (both *ortho* and *para* derivatives) at 20 MHz, 298 and 310 K and pH 7.0 are listed in Table 1 (for GdDO3A-*o*HAP r_1 values are reported at pH 4 and 9). The r_1 values are consistent with the presence of one water molecule in the inner coordination sphere of the metal ion (q = 1), although they are slightly higher than the values measured in analogous conditions for other q = 1 Gd-complexes of comparable molecular weight. For GdDO3A-*o*HAP, the relaxometric properties were studied independently at acid and basic pH (pH 4 and 9) in order to check a possible pH dependence of the relaxometric parameters. Notably, the variable-temperature ^{17}O R_2 profiles of GdDO3A-*o*HAP at both pH (Fig. 1A and Fig. S13, ESI[i]) are clearly different from those of the other Gd-chelates, showing an R_2 decrease with increasing T.

Table 1. Best-fit parameters obtained from the analysis of the $1/T_1$ ^{1}H NMRD profiles (298 K) and ^{17}O NMR data for GdHPDO3A,[a] GdDO3A-AP, GdDO3A-*o*HAP (at pH 4 and 9) and GdDO3A-*p*HAP[b].

Parameter	Isom.	GdHPDO3A	GdDO3A-AP	GdDO3A-*o*HAP (pH 4)	GdDO3A-*o*HAP (pH 9)	GdDO3A-*p*HAP
$r_1^{298}(\mathrm{mM^{-1}s^{-1}})^c$		4.6	5.1 ± 0.1	6.4 ± 0.2	6.4 ± 0.2	5.8 ± 0.1
$r_1^{310}(\mathrm{mM^{-1}s^{-1}})^c$		3.6	4.6 ± 0.1	5.4 ± 0.3	4.9 ± 0.3	4.9 ± 0.2
τ_R^{298}(ps)		65	100 ± 2	105 ± 3	105 ± 3	95 ± 5
τ_M^{298}(ns)	SAP	640	1200 ± 20	210 ± 5	256 ± 12	950 ± 10
	TSAP	8.9	25 ± 2	2.2 ± 0.1	4.7 ± 5	7.1 ± 0.7
Δ^2 (10^{19} s^{-2})	SAP	9.9	9.8 ± 0.3	8.5 ± 0.5	4.7 ± 0.5	7.0 ± 0.3
	TSAP	1.5	5.0 ± 0.2	3.0 ± 0.4	3.2 ± 0.3	3.3 ± 0.2
τ^{298}_V (ps)	SAP	8	5.1 ± 0.1	5.7 ± 0.2	6.5 ± 0.3	5.8 ± 0.1
	TSAP	30	14.8 ± 0.3	24.8 ± 0.3	30.0 ± 0.5	3.4 ± 0.2
E_M (kJ mol^{-1})	SAP	53	50 ± 2	34 ± 2	37 ± 2	54 ± 3
	TSAP	15	27 ± 1	40 ± 1	39 ± 1	32 ± 2

[a] From ref. 13. [b] The parameters fixed in the fitting procedure are: q = 1, r_{GdO} = 2.5 Å, r_{GdH} = 3.0 Å, a_{GdH} = 4.0 Å, $^{298}D_{GdH}$ = 2.25 × 10^{-5} cm^2 s^{-1}, E_R = 1.6 kJ mol^{-1}, E_v = 1 kJ mol^{-1}, $A/\hbar$ = −3.6 × 10^6 rad s^{-1}. [c] 20 MHz.

For all complexes, the presence of two species with very different water exchange dynamics can be envisaged by the shapes of the curves that are distant from the simple pseudo-exponential decay expected for systems containing one coordinated water molecule in exchange with bulk solvent. Thus, we considered the presence in solution of the SAP and TSAP isomers observed in the ^{1}H NMR spectra of the corresponding Eu-complexes. Similar observations were recently reported for GdHPDO3A,[13] a hydroxyphenyl derivative of GdHPDO3A,[14] and previously for two GdDOTA–bisamide complexes[15] showing that the TSAP isomer,

present in lower concentration, has a τ_M ($\tau_M = 1/k_{ex}$) significantly shorter than that observed for the SAP isomer. The variable-temperature ^{17}O R_2 profiles were fitted according to the well-established set of Swift–Connick equations[16] using a model that considers the presence in solution of two isomeric species whose relative population is extrapolated from the ^1H NMR spectra of the Eu-complexes (the TSAP/SAP ratio is considered constant over the range of temperatures under examination, Fig. S7–S10, ESI[i]). Moreover, the Nuclear Magnetic Resonance Dispersion (NMRD, Fig. S12, ESI[i]) data were analysed using the standard Solomon Bloembergen Morgan model for the inner-sphere relaxation mechanism[17] and Freed's model for the outer-sphere components[18] considering a weighted average of the values obtained for the two isomers by fitting the ^{17}O NMR data (Table 1). The rotational correlation time τ_R, considering that two isomers have similar rotational dynamics, was determined for all complexes by fitting the NMRD profiles. Values in the range 90–105 ps were found, in line with τ_R values obtained for Gd-complexes of analogous molecular volume.[1] The fitting data were compared in Table 1 to the parameters reported for GdHPDO3A in which the model for the two isomeric species was also considered. The results show a fast k_{ex} for all TSAP isomers (τ_M ranges from 2.2 to 25 ns) but a marked difference in the τ_M of the SAP isomer of GdDO3A-*o*HAP (≈200 ns) with respect to the other Gd-complexes (≈1 μs). Notably, this fast k_{ex} for the SAP isomer GdDO3A-*o*HAP does not change with pH and thus passing from a neutral to an anionic complex. The fast k_{ex} for GdDO3A-*o*HAP clearly suggests that, in solution, the 2-hydroxyacetophenone moiety must be *cis* conformation and the *o*-phenolic OH involved in the k_{ex} acceleration. This is maybe due to solvent assisted H-bonding to the coordinated water molecule, as shown by the *cis* conformation of the crystal structure (Fig. S5, ESI[i]). Notably, in case of GdDO3A-*p*HAP, when the OH points outside the coordination cage, the k_{ex} of the SAP isomer is slow as in case of the simple acetophenone system, or Ln^{III}–DOTA-derivatives having ketone donor pendant arms.[19]

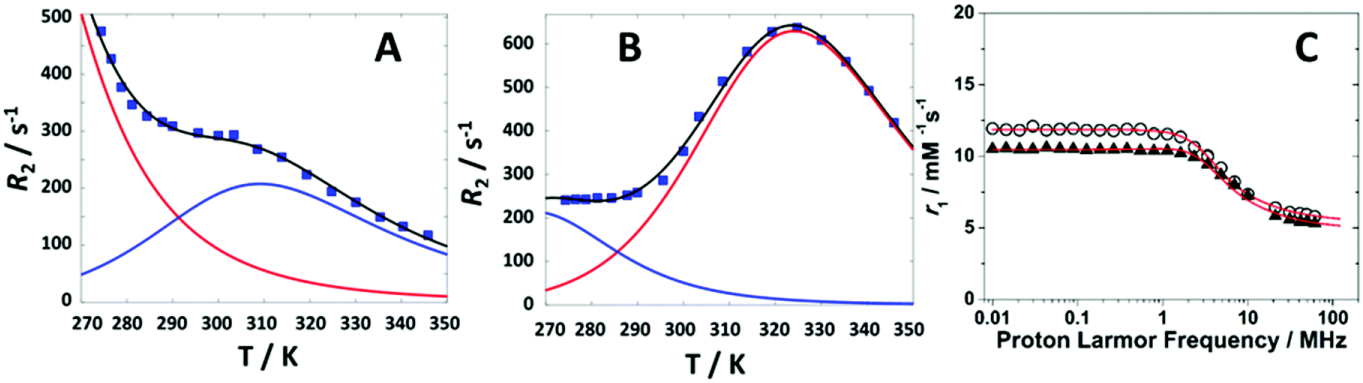

Fig. 1. Transverse ^{17}O relaxation rates measured at 11.74 T for (A) GdDO3A-*o*HAP at pH 9, 13.1 mM and (B) for GdDO3A-*p*HAP at pH 7, 19.2 mM. The red and blue lines represent the calculated contributions of the isomeric species SAP and TSAP, respectively. (C) ^1H NMRD profiles recorded at 298 for GdDO3A-*o*HAP at pH 9 (empty circles) and GdDO3A-*p*HAP at pH 7 (black triangles).

A Density Functional Theory (DFT) study was performed to gain further insight into the fast water exchange observed for the SAP isomer of GdDO3A-*o*HAP. Thus, the structures of the SAP isomers of GdDO3A-AP and deprotonated GdDO3A-*o*HAP were optimized at the M062X/LCRECP/6-311G(d,p)[20,21] level (see computational details in ESI[i]). The model systems investigated included a few second-sphere water molecules, which are crucial for a proper description of the Gd–O_{water} distances and spin-density distributions.[22] Bulk solvent effects were considered by using a polarizable continuum model. The optimized geometry of the GdDO3A-*o*HAP system presents a slightly longer Gd–O_{water} distance (2.503 Å) than GdDO3A-AP (2.469 Å). The exchange of the coordinated water molecule with bulk water in this type of complexes follows a dissociative mechanism, and thus a longer Gd–O_{water} distance anticipates a faster water

exchange.[23] The coordinated water molecule in GdDO3A-*o*HAP is involved in hydrogen-bonding interaction with the oxygen atom of the phenolate group. The water exchange reaction in these complexes was further investigated by locating the transition states (TS) connecting the nine-coordinate complexes and the eight-coordinate intermediate generated in a dissociative pathway (Fig. 2). The Gd···O_{water} distances in these TSs are much more different than in case of the fundamental state, being 3.606 and 3.436 Å for GdDO3A-AP and GdDO3A-*o*HAP, respectively. In GdDO3A-*o*HAP the water molecule leaving the Gd^{III} coordination environment is hydrogen-bonded to the phenolate group, which stabilizes the eight-coordinate transition state. The activation free energies ($\Delta G^{\#298}$) obtained with DFT (36.3 and 21.8 kJ mol^{-1} for GdDO3A-AP and GdDO3A-*o*HAP, respectively) further confirm the TS stabilization. Thus, intramolecular hydrogen-bonding interactions with the peripheral phenolate group favour the exchange of the coordinated water molecule, thereby accelerating k_{ex}. The analysis of the activation enthalpies ($\Delta H^{\#}$) and entropies ($\Delta S^{\#}$) provides additional insight into the reasons behind the fast water exchange rate in GdDO3A-*o*HAP. For GdDO3A-AP our DFT calculations provide $\Delta H^{\#}$ = 42.0 kJ mol^{-1} and $\Delta S^{\#}$ = +19.2 J mol^{-1} K^{-1}. Positive $\Delta S^{\#}$ values are expected for a dissociatively activated mechanism. In the case of GdDO3A-*o*HAP we obtained $\Delta H^{\#}$ = 17.4 kJ mol^{-1} and $\Delta S^{\#}$ = −14.8 J mol^{-1} K^{-1}. The lower $\Delta H^{\#}$ value obtained for GdDO3A-*o*HAP is likely the result of (i) a weaker (longer) Gd–O_{water} bond, and (ii) the strengthening of the hydrogen-bonding interaction involving the departing water molecule and the phenolate oxygen atom on moving from the ground to the transition state. The low $\Delta H^{\#}$ in GdDO3A-*o*HAP is compensated in part by an unfavourable entropy contribution, which we ascribe to the formation of an ordered hydrogen bonding network in the TS of GdDO3A-*o*HAP (involving the departing water molecule, the phenolate oxygen atom and second-sphere water molecules). The DFT calculations have known limitations, in particular regarding the accuracy of the entropy contributions, given the limited number of explicit water molecules included in the model. Nevertheless, they strongly support the stabilization of the TS through H-bond, with consequent lowering of the energy barrier and acceleration of the water exchange reaction in GdDO3A-*o*HAP. This effect is rather common in biochemistry and catalysis, as for instance in the amide bond-formation process.[24]

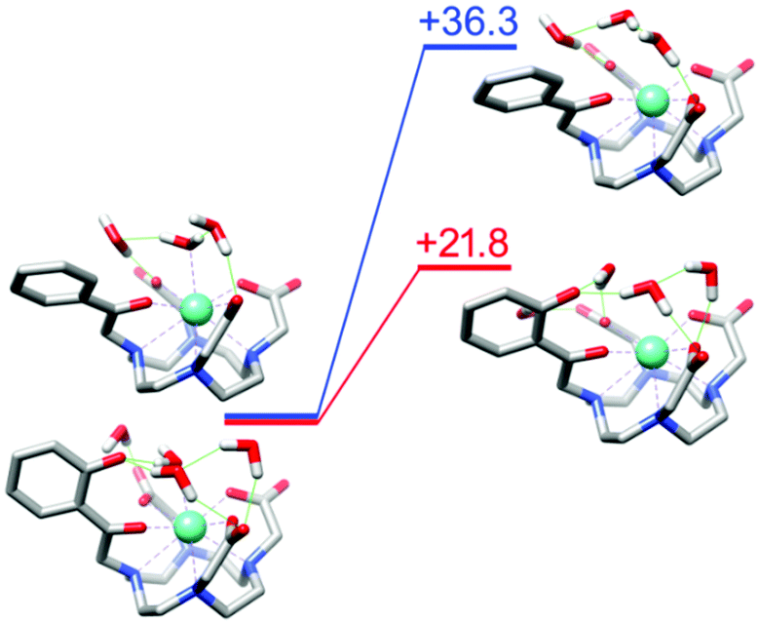

Fig. 2. Structures of the local energy minima (left) and transition states (right) characterizing the dissociative water exchange mechanism in GdDO3A-AP and GdDO3A-*o*HAP. The numbers represent the calculated activation free energies in kJ mol^{-1}.

Interestingly, the reduction of the ketone to hydroxyl group in GdHPDO3A-phenol chelate reported recently[9,14] did not result in an increase of the k_{ex}.[14] However, intramolecular H-bonding between the coordinated hydroxyl group and the phenolate group generated a relaxivity increase due to proton exchange.[9] Therefore, we can highlight that the acceleration of k_{ex} requires not only H-bond between the coordinated water molecule and the phenolate oxygen, but also a conjugated sp^2*ortho*-hydroxyacetophenone system.

In conclusion, we have shown that hydrogen bonds involving the coordinated water molecule and heteroatoms in the periphery of the water binding site can accelerate water exchange rate by an order of magnitude. As a result, both the SAP and TSAP isomers of GdDO3A-*o*HAP present very high k^{298}_{ex} values. These results pave the way to the development of more efficient Gd^{III}-based contrast agents, as fast water exchange rates are required to attain high relaxivities, particularly for slowly tumbling systems. This issue can be of key importance to reduce the Gd^{III}-doses used for MRI scans in clinical practice, which would minimize the risks associated to Gd^{III} toxicity.

This work was carried out under the EU COST Action CA15209 "European Network on NMR Relaxometry". The authors thank Centro de Supercomputación de Galicia (CESGA) for providing the computer facilities.

Conflicts of interest

There are no conflicts to declare.

References

01 (*a*) *The Chemistry of Contrast Agents in Medical Magnetic Resonance Imaging*, A. E. Merbach, L. Helm and E. Toth, John Wiley & Sons Ltd, 2013; (*b*) L. Helm and J. R. Morrow, *et al.*, *Contrast Agents for MRI: Experimental Methods*, V. C. Pierre and M. J. Allen, The Royal Society of Chemistry, 2018, pp. 121–242.

02 (*a*) B. N. Siriwardena-Mahanama and M. J. Allen, *Molecules*, 2013, **18**, 9352; (*b*) S. Aime, M. Botta, M. Fasano and E. Terreno, *Acc. Chem. Res.*, 1999, **32**, 941.

03 (*a*) S. Aime, M. Botta, M. Fasano, M. P. M. Marques, C. F. G. C. Geraldes, D. Pubanz and A. E. Merbach, *Inorg. Chem.*, 1997, **36**, 2059; (*b*) M. Woods, S. Aime, M. Botta, J. A. K. Howard, J. M. Moloney, M. Nave, D. Parker, M. Port and O. Rousseaux, *J. Am. Chem. Soc.*, 2000, **122**, 9781.

04 (*a*) F. A. Dunand, S. Aime and A. E. Merbach, *J. Am. Chem. Soc.*, 2000, **122**, 1506; (*b*) F. A. Dunand, R. S. Dickins, D. Parker and A. E. Merbach, *Chem. – Eur. J.*, 2001, **7**, 5160.

05 R. Ruloff, E. Toth, R. Scopelliti, R. Tripier, H. Handel and A. E. Merbach, *Chem. Commun.*, 2002, 2630.

06 (*a*) S. Laus, R. Ruloff, E. Toth and A. E. Merbach, *Chem. – Eur. J.*, 2003, **9**, 3555; (*b*) L. Tei, G. Gugliotta, Z. Baranyai and M. Botta, *Dalton Trans.*, 2009, 9712.

07 (*a*) E. Balogh, M. Mato-Iglesias, C. Platas-Iglesias, E. Toth, K. Djanashvili, J. A. Peters, A. de Blas and T. Rodríguez-Blas, *Inorg. Chem.*, 2006, **45**, 8719; (*b*) J. Kotek, P. Lebduskova, P. Hermann, L. Vander Elst, R. N. Muller, C. F. G. C. Geraldes, T. Maschmeyer, I. Lukes and J. A. Peters, *Chem. – Eur. J.*, 2003, **9**, 5899.

08 E. Boros, R. Srinivas, H.-K. Kim, A. M. Raitsimring, A. V. Astashkin, O. G. Poluektov, J. Niklas, A. D. Horning, B. Tidos and P. Caravan, *Angew. Chem., Int. Ed.*, 2017, **56**, 5603.

09 I. M. Carnovale, M. L. Lolli, S. C. Serra, A. F. Mingo, R. Napolitano, V. Boi, N. Guidolin, L. Lattuada, F. Tedoldi, Z. Baranyai and S. Aime, *Chem. Commun.*, 2018, **54**, 10056.

10 A. Beeby, L. M. Bushby, D. Maffeo and J. A. G. Williams, *J. Chem. Soc., Dalton Trans.*, 2002, 48.

11 (*a*) M. Woods, G. E. Kiefer, S. Bott, A. Castillo-Muzquiz, C. Eshelbrenner, L. Michaudet, K. McMillan, S. D. K. Mudigunda, D. Ogrin, G. Tircso, S. Zhang, P. Zhao and A. D. Sherry, *J. Am. Chem. Soc.*, 2004, **126**, 9248; (*b*) G. B. Giovenzana, R. Negri, G. A. Rolla and L. Tei, *Eur. J. Inorg. Chem.*, 2012, 2035.

12 C. Adair, M. Woods, P. Zhao, A. Pasha, P. M. Winter, G. M. Lanza, P. Athey, A. D. Sherry and G. E. Kiefer, *Contrast Media Mol. Imaging*, 2007, **2**, 55.

13 D. Delli Castelli, M. C. Caligara, M. Botta, E. Terreno and S. Aime, *Inorg. Chem.*, 2013, **52**, 7130.

14 A. Fringuello Mingo, S. Colombo Serra, S. Baroni, C. Cabella, R. Napolitano, I. Hawala, I. M. Carnovale, L. Lattuada, F. Tedoldi and S. Aime, *Magn. Reson. Med.*, 2017, **78**, 1523.

15 (*a*) S. Zhang, Z. Kovacs, S. Burgess, S. Aime, E. Terreno and A. D. Sherry, *Chem. – Eur. J.*, 2001, **7**, 288; (*b*) A. Pagoto, R. Stefania, F. Garello, F. Arena, G. Digilio, S. Aime and E. Terreno, *Bioconjugate Chem.*, 2016, **27**, 1921.

16 T. J. Swift and R. E. Connick, *J. Chem. Phys.*, 1962, **37**, 307.

17 (*a*) I. Solomon and N. Bloembergen, *J. Chem. Phys.*, 1956, **25**, 261; (*b*) N. Bloembergen and L. O. Morgan, *J. Chem. Phys.*, 1961, **34**, 842.

18 J. H. Freed *J. Chem. Phys.*, 1978, **68**, 4034.

19 K. N. Green, S. Viswanathan, F. A. Rojas-Quijano, Z. Kovacs and A. D. Sherry, *Inorg. Chem.*, 2011, **50**, 1648.

20 Y. Zhao and D. G. Truhlar, *Theor. Chem. Acc.*, 2008, **120**, 215.

21 M. Dolg, H. Stoll, A. Savin and H. Preuss, *Theor. Chim. Acta*, 1989, **75**, 173.

22 D. Esteban-Gomez, A. de Blas, T. Rodriguez-Blas, L. Helm and C. Platas-Iglesias, *ChemPhysChem*, 2012, **13**, 3640.

23 M. Regueiro-Figueroa and C. Platas-Iglesias, *J. Phys. Chem. A*, 2015, **119**, 6436.

24 A. Rimola, M. Sodupe and P. Ugliengo, *J. Phys. Chem. C*, 2016, **120**, 24817.

[i] Electronic supplementary information (ESI) available: Experimental details, crystallographic data, spectroscopic data and geometries obtained with DFT. CCDC 1875349. For ESI and crystallographic data in CIF or other electronic format see DOI: 10.1039/c8cc08556k.